

# Unique Numerical Scheme for a Modified Equation of Fluid Motion: Approaching New Solver Development to a Fundamental Flow Problem

Bo Wan\*, Friedrich Karl Benra and Hans Josef Dohmen

Department of Mechanical Engineering, Faculty of Engineering Sciences  
University of Duisburg-Essen  
Keetmanstr. 3-9, 47058 Duisburg, GERMANY  
Tel: 0049-203-379-3013 Fax: 0049-203-379-3038  
email: [bo.wan@stud.uni-due.de](mailto:bo.wan@stud.uni-due.de)

Accepted 21<sup>th</sup> January, 2013

## Abstract

On the basis of a scale-invariant model of statistical mechanics, the scale-invariant form of the equation of motion was introduced by Sohrab recently. This newly modified equation of fluid motion owns linear properties and is almost identical to the classical Navier-Stokes equations for solving flow problems. In order to dig potential advantages of this modified equation in engineering applications, the current paper goes deeper insights into the modified equation of fluid motion by the numerical method. In Open FOAM environment, a numerical solver was developed to employ this modified equation to solve engineering flow problems. After the finite volume method discretisation was carried out, the resulted algebraic equations derived from the modified equation were linear. Hence another technique was assigned to the developed solver to improve the iteration procedure. As an application example, the laminar boundary layer flow over a flat plate was resolved by the developed solver. Comparing the obtained results with those of the Navier-Stokes solver and measurement, it is found that the developed solver produced reasonable predictions for this fundamental flow problem, and consumed much less computational time than the Navier-Stokes due to the linear properties. Such results conclude that the developed solver is more efficient than the current ones solving the Navier-Stokes equations.

**Keywords:** Modified Equation of Fluid Motion, Statistical Mechanics, CFD, Navier-Stokes Equations, Flat Plate

## 1.0 Introduction

Computational fluid dynamics (CFD) methodologies are widely used by engineers and designers in a broad range of industries to gain deeper insight into the impact of fluid dynamics on the design process. The fundamental governing equations of almost all CFD problems are the Navier-Stokes equations. Under most conditions, the expression of these equations is second order, non-homogenous, non-linear and partial differential. These properties, especially the non-linear properties, increase the associated computational cost and impede the development of numerical solutions obtained using the Navier-Stokes equations. Therefore another equation which does not have non-linear properties will greatly interest the industry.

Continuum mechanics scales are characterized by the condition  $Kn \ll 1$ . Golse (2011) discussed the derivation

of the Navier-Stokes equations for incompressible flow from the Boltzmann equation, thus pointing out the application of the Boltzmann equation in fluid dynamics. Similarly, on the basis of a scale-invariant model of statistical mechanics, Sohrab (1999a) introduced the derivation of a linear equation from the scale-invariant form of the Boltzmann equation, using a scale-invariant definition of the convective velocity.

This linear equation is termed the "scale-invariant form of the equation of motion" or the "modified equation of fluid motion". Preliminary studies done by Sohrab et al. (Sohrab, 1999b, 2005, 2008a; Benra and Sohrab, 2006; Inkman and Sohrab, 2008) have shown that this modified equation can be applied to incompressible flow problems. Several basic flow models were analytically investigated by using this equation. Consequently, satisfactory correlation between the estimated and experimental data was achieved. This result stimulated the application of the modified equation of fluid motion in CFD problems. The linear property of the modified equation of fluid motion allows users to develop an efficient numerical solver to simulate flow problems. The associated iteration of the solver could be simplified because linear discrete algebraic equations are obtained after the finite volume method (FVM) discretisation is carried out. As compared to the current numerical solvers solving the Navier-Stokes equations, the new solver will reduce the required computational resources and the corresponding calculation time. In the current paper, the modified equation of fluid motion for incompressible flow is under consideration.

The derivation process and FVM discretization of the modified equation are discussed in detail. On the basis of these discussions, a numerical solver is then developed by using Open field operation and manipulation (OpenFOAM) to exert the linear advantages of the modified equation of fluid motion in CFD applications. Moreover this solver is applied to solve the fundamental flow model of a laminar boundary layer flow over a flat plate.

## 2.0 Scale-invariant model of statistical mechanics and modified equation of fluid motion

Sohrab (1999a) introduced the physical and mathematical foundation of a scale-invariant statistical theory. The

appearance of this theory offers another understanding for the natural phenomena in many branches of the modern science. The construction of the associated mathematical models would be greatly helpful to some fundamental conceptual difficulties which are encountered in engineering applications.

**2.1 Scale-invariant model of statistical mechanics**

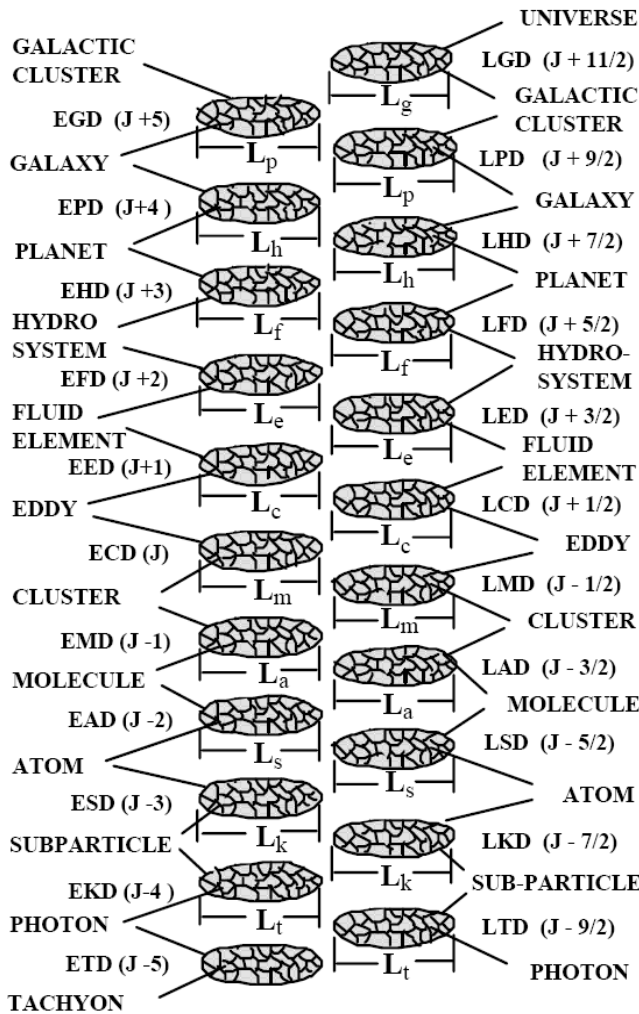


**Figure 1.** A scale-invariant view of statistical mechanics from cosmic to tachyonic scales (Sohrab, 1999a)

A scale-invariant model was established for both equilibrium statistical mechanics, which is governed by the Gibbs function, and non-equilibrium field, which is based on the Liouville, Boltzmann and Maxwell methods. As shown in Fig. 1, the broad scales from the exceedingly large scale of cosmic to the minute scale of quantum optics are included in the scale-invariant model (Sohrab, 1999a). According to statistical mechanics, each field, described by a distribution function

$$f_{\beta}(\mathbf{r}_{\beta}, t_{\beta}, \mathbf{u}_{\beta}) \tag{1}$$

defines a “system”, which is composed of an ensemble of “element”, as well, each element is composed of an ensemble of small particles viewed as point mass “atoms”. The element (system) of the smaller scale ( $j$ ) becomes the atom (element) of the larger scale ( $j+1$ ). Following the classical method

(Sohrab, 1999a), the invariant definitions of the density  $\rho_{\beta}$ , velocity of element  $\mathbf{U}_{\beta}$ , atom and system at scale  $\beta$  can be written as

$$\rho_{\beta} = n_{\beta} m_{\beta} = m_{\beta} \int f_{\beta} d\mathbf{u}_{\beta} \tag{2}$$

$$\mathbf{u}_{\beta} = \mathbf{U}_{\beta-1}, \mathbf{u}_{\beta+1} = \mathbf{U}_{\beta} \tag{3}$$

$$\mathbf{U}_{\beta} = \rho_{\beta}^{-1} m_{\beta} \int \mathbf{u}_{\beta} f_{\beta} d\mathbf{u}_{\beta} \tag{4}$$

$$\mathbf{w}_{\beta} = \mathbf{U}_{\beta+1} \tag{5}$$

As discussed in (Sohrab, 1999a), the invariant definition of the peculiar velocity  $\mathbf{v}'_{\beta}$  arises from the mechanical potential energy in non-equilibrium statistical mechanics as follows:

$$\varepsilon = 3kT = \frac{m_{\beta} \mathbf{v}'_{\beta}{}^2}{2} \tag{6}$$

This peculiar velocity is related to  $\mathbf{u}_{\beta}$  and  $\mathbf{U}_{\beta}$

$$\mathbf{v}'_{\beta} = \mathbf{u}_{\beta} - \mathbf{U}_{\beta} \tag{7}$$

Then, going to the higher scale  $\beta+1$ , we have

$$\mathbf{v}'_{\beta+1} = \mathbf{u}_{\beta+1} - \mathbf{U}_{\beta+1} \tag{8}$$

Substituting Eqs. (3) and (5) into Eq. (8) gives

$$\mathbf{v}'_{\beta+1} = \mathbf{U}_{\beta} - \mathbf{w}_{\beta} \tag{9}$$

At scale  $\beta$ , the system velocity  $\mathbf{w}_{\beta}$  can also be understood as the convective velocity

$$\mathbf{w}_{\beta} = \langle \mathbf{U}_{\beta} \rangle \tag{10}$$

Replacing  $\mathbf{v}'_{\beta+1}$  by the diffusion velocity  $\mathbf{v}_{\beta gh}$ , at the current scale  $\beta$ , we have the local velocity expressed as the sum of convective velocity and diffusion velocity

$$\mathbf{U}_{\beta} = \mathbf{w}_{\beta} + \mathbf{v}_{\beta gh} \tag{11}$$

Where

$$\mathbf{v}_{\beta gh} = \mathbf{v}_{\beta g} + \mathbf{v}_{\beta h} \tag{12}$$

For most flow problems, the fluid diffusion contains two components. In detail,

$$\mathbf{v}_{\beta g} = -D_{\beta} \nabla \ln(\rho_{\beta}) \tag{13}$$

which is related to the density dependent diffusion, and

$$\mathbf{v}_{\beta h} = -\nu_{\beta} \nabla \ln(\mathbf{U}_{\beta}) \quad (14)$$

which stands for the viscous influence to the diffusion. For incompressible flow, only the viscous diffusion is under consideration. Hence Eq. (11) can be simplified to

$$\mathbf{U}_{\beta} = \mathbf{w}_{\beta} + \mathbf{v}_{\beta h} \quad (15)$$

Eq. (15) plays a significant role in the derivation of the modified equation of fluid motion from the scale-invariant form of the Boltzmann equation.

## 2.2 Modified equation of fluid motion

Fluid dynamic regimes are characterized by the condition  $\text{Kn} \ll 1$ . Golse (2011) discussed the derivation of the Navier-Stokes equations for incompressible flow from the Boltzmann equation, thus pointing out the application of the Boltzmann equation in fluid dynamics. In the scale-invariant model as shown in Fig. 1, the classical fluid mechanics covers the range LFD-LCD. At these scales, Sohrab (2008b) gave the derivation of the modified equation of fluid motion from the scale-invariant form of the Boltzmann equation, using a scale-invariant definition of convective velocity. On the basis of the theory of non-equilibrium statistical mechanics, the scale-invariant form of the Boltzmann equation in the absence of body force is

$$\frac{\partial f_{\beta}}{\partial t} + \mathbf{U}_{\beta} \cdot \nabla f_{\beta} = \frac{\delta f_{\beta}}{\delta t} \quad (16)$$

Multiplying Avogadro-Loschmidt number with an arbitrary invariant function of velocity  $\Psi_{\beta}$  and integrating them to both sides of Eq. (16), we obtain the invariant Enskog equation of change

$$\frac{\partial}{\partial t} (n_{\beta} \cdot \overline{\Psi_{\beta}}) + \nabla \cdot (n_{\beta} \cdot \overline{\Psi_{\beta} \mathbf{U}_{\beta}}) = \int \Psi_{\beta} \cdot \frac{\delta f_{\beta}}{\delta t} d\mathbf{U}_{\beta} \quad (17)$$

Defining  $\Psi_{\beta}$  in Eq. (17) as the invariant form of momentum

$$\Psi_{\beta} = m_{\beta} \mathbf{U}_{\beta} \quad (18)$$

we have

$$\begin{aligned} & \frac{\partial}{\partial t} (n_{\beta} \cdot m_{\beta} \mathbf{U}_{\beta}) + \nabla \cdot (n_{\beta} \cdot m_{\beta} \mathbf{U}_{\beta} \mathbf{U}_{\beta}) \\ & = \int m_{\beta} \mathbf{U}_{\beta} \cdot \frac{\delta f_{\beta}}{\delta t} d\mathbf{U}_{\beta} \end{aligned} \quad (19)$$

By considering the definition of density

$$n_{\beta} \cdot m_{\beta} = \rho_{\beta} \quad (20)$$

we see that Eq. (19) can be written as

$$\frac{\partial}{\partial t} (\rho_{\beta} \mathbf{U}_{\beta}) + \nabla \cdot (\rho_{\beta} \mathbf{U}_{\beta} \mathbf{U}_{\beta}) = \int m_{\beta} \mathbf{U}_{\beta} \cdot \frac{\delta f_{\beta}}{\delta t} d\mathbf{U}_{\beta} \quad (21)$$

According to Sohrab (2008b), under the Stokes assumption, the term at the right hand side (RHS) of Eq. (21) results in

$$\int m_{\beta} \mathbf{U}_{\beta} \cdot \frac{\delta f_{\beta}}{\delta t} d\mathbf{U}_{\beta} = -\nabla p_{\beta} + \frac{1}{3} \mu \nabla (\nabla \cdot \mathbf{U}_{\beta}) \quad (22)$$

which shows the thermodynamic and hydrodynamic pressure. For incompressible flow, the hydrodynamic pressure can be neglected, hence Eq. (21) is simplified as

$$\rho_{\beta} \cdot \frac{\partial}{\partial t} \mathbf{U}_{\beta} + \rho_{\beta} \nabla \cdot (\mathbf{U}_{\beta} \mathbf{U}_{\beta}) = -\nabla p_{\beta} \quad (23)$$

Referring to Eq. (15) in the previous section, we see that the second term in Eq. (23) can be expanded as

$$\begin{aligned} \rho_{\beta} \nabla \cdot (\mathbf{U}_{\beta} \mathbf{U}_{\beta}) &= \rho_{\beta} \nabla \cdot [(\mathbf{w}_{\beta} + \mathbf{v}_{\beta h}) \mathbf{U}_{\beta}] \\ &= \rho_{\beta} \nabla \cdot (\mathbf{w}_{\beta} \mathbf{U}_{\beta}) + \rho_{\beta} \nabla \cdot (\mathbf{v}_{\beta h} \mathbf{U}_{\beta}) \end{aligned} \quad (24)$$

Since the convective velocity can be considered as a constant for the local flow field, Eq. (24) can be transferred as

$$\rho_{\beta} \nabla \cdot (\mathbf{U}_{\beta} \mathbf{U}_{\beta}) = \rho_{\beta} \mathbf{w}_{\beta} \nabla \mathbf{U}_{\beta} + \rho_{\beta} \nabla \cdot (\mathbf{v}_{\beta h} \mathbf{U}_{\beta}) \quad (25)$$

Considering Eq.(14), we can expand the second term on the RHS of Eq. (25) as

$$\begin{aligned} \rho_{\beta} \nabla \cdot (\mathbf{v}_{\beta h} \mathbf{U}_{\beta}) &= \rho_{\beta} \nabla \cdot \{[-\nu_{\beta} \nabla \ln(\mathbf{U}_{\beta})] \mathbf{U}_{\beta}\} \\ &= -\rho_{\beta} \nu_{\beta} \nabla \cdot \left[ \left( \frac{1}{\mathbf{U}_{\beta}} \nabla \mathbf{U}_{\beta} \right) \mathbf{U}_{\beta} \right] \\ &= -\rho_{\beta} \nu_{\beta} \nabla^2 \mathbf{U}_{\beta} \end{aligned} \quad (26)$$

Then, substituting Eq. (26) into Eq. (25) gives

$$\rho_{\beta} \nabla \cdot (\mathbf{U}_{\beta} \mathbf{U}_{\beta}) = \rho_{\beta} \mathbf{w}_{\beta} \nabla \mathbf{U}_{\beta} - \rho_{\beta} \nu_{\beta} \nabla^2 \mathbf{U}_{\beta} \quad (27)$$

Substituting Eq. (27) into Eq. (23), we have the equation as follows:

$$\frac{\partial}{\partial t} \mathbf{U}_{\beta} + \mathbf{w}_{\beta} \nabla \mathbf{U}_{\beta} - \nu_{\beta} \nabla^2 \mathbf{U}_{\beta} = -\frac{\nabla p_{\beta}}{\rho_{\beta}} \quad (28)$$

which is known as the modified equation of fluid motion for incompressible flow. On the other hand, for compressible flow, this modified equation owns the similar expression. The detailed explanation can be found in (Sohrab 2008b). In Eq. (28), a convective velocity is present. This parameter can be calculated by Eq. (5) or (10). It means that, on one hand, at the current flow scale the convective velocity is equal to the local velocity at the next high scale; on the other hand, it can be understood as the system or average velocity of the flow domain, which can be constructed theoretically for simple flow models. In order to clarify this property, the convective velocity for the laminar boundary layer flow will be discussed in detail in section 4.

## 2.3 Difference between the Navier-Stokes equation and the modified equation of fluid motion

Arising from the Cauchy momentum equation

$$\rho_\beta \cdot \frac{D\mathbf{U}_\beta}{Dt} = \nabla \cdot \boldsymbol{\sigma} + \mathbf{F} \quad (29)$$

he classical Navier-Stokes equations for incompressible flow can be expressed as

$$\frac{\partial}{\partial t} \mathbf{U}_\beta + \mathbf{U}_\beta \nabla \mathbf{U}_\beta - \nu_\beta \nabla^2 \mathbf{U}_\beta = -\frac{\nabla p_\beta}{\rho_\beta} \quad (30)$$

with the consideration of continuity equation

$$\frac{\partial \rho_\beta}{\partial t} + \nabla \cdot (\rho_\beta \mathbf{U}_\beta) = 0 \quad (31)$$

Hence, the Navier-Stokes equations are limited for the continuum mechanics. However for the modified equation of fluid motion (Eq. (28)), the continuity equation is not taken into account, therefore the modified equation would be available for more physical scales. Comparing the second terms on the (left hand side) LHS of Eqs. (28) and (30), we can be found that, in the modified equation of fluid motion, the convective velocity replaces the local velocity. In the mathematical expression, this important feature in the modified equation of fluid motion eliminates its non-linearity and offers more flexibility for the equation solving process. Moreover, this difference between the two equations has significant physical meaning. When the convective velocity is absent in a steady state, the modified equation of fluid motion will still represent the diffusion of the flow. In contrast, when the local velocity is absent in the Navier-Stokes equation, the whole equation will vanish. More details about this comparison can be found in (Sohrab 2008b). As a numerical investigation, the current paper is many focused on the linear advantage of the modified equation of fluid motion. In the following sections, mathematical analysis, followed by a numerical computation for validations, will highlight this advantage.

### 3.0 FVM discretisation

The modern method to solve the Navier-Stokes equations for CFD problems is to use the finite volume method to represent this equation in the form of the algebraic equations with variables at discrete grid points. After the space discretisation is carried out, the convection acceleration component in the Navier-Stokes equations leads to a quadratic expression in velocity, thus resulting in non-linear algebraic equations. These non-linear components increase the complexity of the velocity coefficient matrixes. Furthermore solving these matrixes requires more computational recourses. In contrast, the discrete form of the modified equation of fluid motion results in the linear expression of the local velocity. This important difference between the two equations will be discussed in detail in this section.

### 3.1 1D discretisation

To clarify the difference mentioned above, a one-dimensional (1D) case is taken as an example to show the discretisation process of the modified equation of fluid motion. For CFD problems, in a steady state, Eq. (28) results in

$$w_\beta \frac{dU_\beta}{dx} - \nu_\beta \frac{d^2U_\beta}{dx^2} = -\frac{dp'_\beta}{dx} \quad (32)$$

Where

$$p'_\beta = \frac{P_\beta}{\rho_\beta} \quad (33)$$

The 1D grids are shown in Fig. 2. Due to the velocity-pressure coupling effect,  $w$  and  $e$  are treated as nodes and  $W, P$  and  $E$  are assumed as the cell centers.

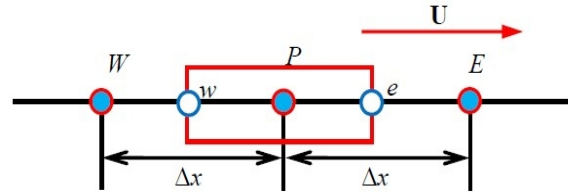


Figure 2. 1D grids

Noting the space discretisation suggestion in Patankar (1980), integrating Eq. (32) in the control volume, we have

$$[(w_\beta A U_\beta)_e - (w_\beta A U_\beta)_w] - \nu [A \frac{dU_\beta}{dx}]_e - (A \frac{dU_\beta}{dx})_w = -[(A p'_\beta)_e - (A p'_\beta)_w] \quad (34)$$

Transferring the velocity coefficients with the pre-defined values at the cell centers gives

$$[(\frac{1}{2} w_P A_P - \frac{1}{2} w_W A_W) U_e - (\frac{1}{2} w_E A_E - \frac{1}{2} w_P A_P) U_w] - \nu [(A_e \frac{U_E - U_P}{\delta x_{PE}} - A_w \frac{U_P - U_W}{\delta x_{WP}})] = A_w p'_w - A_e p'_e \quad (35)$$

Let  $U_w > 0, U_e > 0$ . Taking the upwind scheme, we have

$$U_e = U_P \quad (36)$$

$$U_w = U_W \quad (37)$$

Then, substituting Eqs. (36) and (37) into the LHS of Eq. (35) gives

$$(\frac{1}{2} w_P A_P - \frac{1}{2} w_W A_W + \nu \frac{A_e}{\delta x_{PE}} + \nu \frac{A_w}{\delta x_{WP}}) U_P + (\frac{1}{2} w_P A_P - \frac{1}{2} w_E A_E - \nu \frac{A_w}{\delta x_{WP}}) U_W - \nu \frac{A_e}{\delta x_{PE}} U_E$$

where the coefficient of  $U_P$  contains the convective velocity  $w$  instead of the local velocity  $U$ . Let

$$a_P = \frac{1}{2} w_P A_P - \frac{1}{2} w_W A_W + \nu \frac{A_e}{\delta x_{PE}} + \nu \frac{A_w}{\delta x_{WP}} \quad (38)$$

$$a_W = \frac{1}{2} w_P A_P - \frac{1}{2} w_E A_E - \nu \frac{A_w}{\delta x_{WP}} \quad (39)$$

$$a_e = -\nu \frac{A_e}{\delta x_{PE}} \quad (40)$$

Finally, the discretisation of the modified equation of fluid motion on 1D grids gives

$$a_p \cdot U_p + a_e \cdot U_e + a_w \cdot U_w = A_e p'_e - A_w p'_w \quad (41)$$

Therefore, the difference of the discretisation results between the Navier-Stokes equation and the modified equation of fluid motion is only the coefficient of UP. Defining  $a_p'$  to express this coefficient in the Navier-Stokes equation, we have

$$a_p' = \frac{1}{2} U_p A_p - \frac{1}{2} U_w A_w + \nu \frac{A_e}{\delta x_{PE}} + \nu \frac{A_w}{\delta x_{WP}} \quad (42)$$

which contains the velocity at the calculating point P and the velocities at surrounding points. This coefficient leads to a non-linear algebraic equations, and indicates the non-linear properties of the Navier-Stokes equations.

### 3.2 FVM discretisation in OpenFOAM

The open-source CFD toolbox OpenFOAM, is employed to implement the numerical investigation of the modified equation of fluid motion. Using the FVM structure in this software, a new numerical solver based on the modified equation is programmed. The developed solver is named as Sohrab solver. In order to point out the difference between the iterations of both the Sohrab and Navier-Stokes solvers, this section presents a detailed comparison between the velocity and pressure calculations executed by the both solvers.

#### 3.2.1 Navier-Stokes solver

In a steady state, the Navier-Stokes equations for incompressible flow can be expressed as

$$\mathbf{U} \nabla \mathbf{U} - \nu \nabla^2 \mathbf{U} = -\frac{\nabla p}{\rho} \quad (43)$$

After the FVM discretisation is carried out, the LHS of the Eq. (43) is expressed as follows,

$$\mathbf{U} \nabla \mathbf{U} - \nu \nabla^2 \mathbf{U} = a_p' \mathbf{U}_p + \sum_N a_N' \mathbf{U}_N \quad (44)$$

where  $\mathbf{U}_N$  stands for the velocities at the neighboring points of the point P.

As described by Jasak (1996), in OpenFOAM, an important matrix  $H(\mathbf{U})$  is introduced as

$$H(\mathbf{U}) = -\sum_N a_N' \mathbf{U}_N \quad (45)$$

Then, the momentum equation can be constructed as:

$$a_p' \mathbf{U}_p = H(\mathbf{U}) - \nabla p \quad (46)$$

Expressing  $\mathbf{U}$  in the explicit method gives

$$\mathbf{U}_p = \frac{H(\mathbf{U})}{a_p'} - \frac{\nabla p}{a_p'} \quad (47)$$

Integrating the continuity equation on the cell face gives

$$\nabla \cdot \mathbf{U} = \sum_f A \cdot \mathbf{U}_f = 0 \quad (48)$$

Substituting Eq. (47) into Eq. (48), we obtain the pressure equation as follows:

$$\nabla \cdot \left( \frac{1}{a_p'} \nabla p \right) = \sum_f A \cdot \left( \frac{H(\mathbf{U})}{a_p'} \right)_f \quad (49)$$

Eq. (49) helps the solver to compute the pressure (or pressure gradient) with pressure boundary conditions. Then, the velocity  $\mathbf{U}_p$  can be computed by Eq. (47) and updated by iterations until a convergence is achieved.

A simple flow chart can represent this calculation process in OpenFOAM. As shown in Fig. 3, the matrix  $H(\mathbf{U})$  will be updated in each velocity iteration ( $\mathbf{U}_p$  iteration) until the velocity and pressure reach the convergence in the current time step. Using these converged values, the code recalculates the coefficients of  $a_p'$  and  $a_N'$  to initialize the next time step. When the residual of the velocity calculation reaches a limited value, the velocity converges for the whole calculation, and the difference of  $a_p'$  and  $a_N'$  between the neighboring time steps can be neglected. In this method, the non-linear properties of the Navier-Stokes equations are solved by the iteration technology as well as the velocity-pressure coupling.

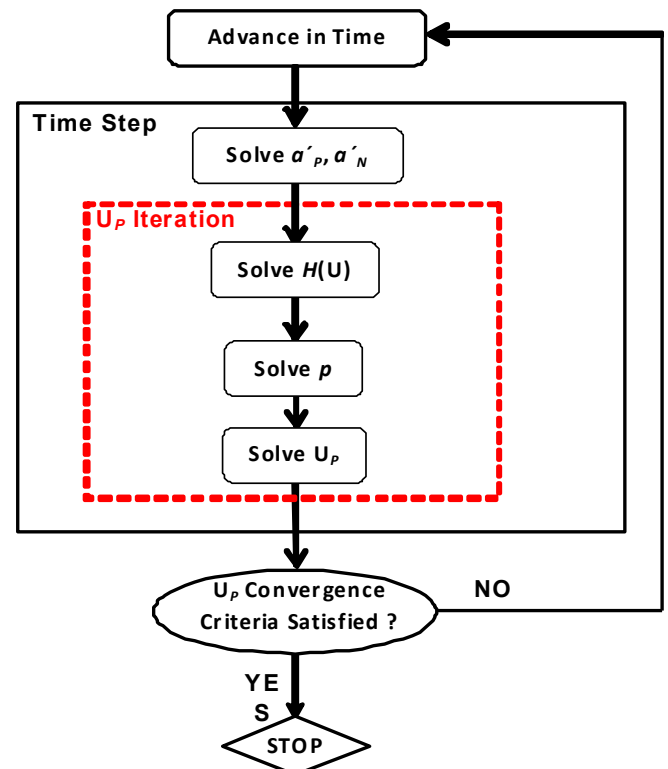


**Figure 3.** Flow chart of the calculation process of the Navier-Stokes solver in OpenFOAM

### 3.2.2 Sohrab solver

The discretisation of the modified equation of fluid motion delivers another expressions of  $a_P$  and  $a_N$ . Noting that these two coefficients are composed of the convective velocity, and independent of the local velocity which is the variable to be solved, we can find that  $a_P$  and  $a_N$  can be directly fixed at the initial step of the FVM computation. Hence, these two coefficients are not necessary to join the time step iterations in the solver. This feature points out the advantage of the linear property of the modified equation of fluid motion in numerical applications. However, the velocity-pressure coupling difficulty exists in the equation, therefore the iteration method is still required when coding the Sohrab solver. Certainly, the iteration of the Sohrab solver is different to that of the Navier-Stokes solver described in Fig. 3. The flow chat in Fig. 4 shows the corresponding new iteration process in the Sohrab solver. Comparing the FVM computation processes of the two solvers, we can find that the Sohrab solver saves the re-calculation process of the coefficients  $a_P$  and  $a_N$  in each time step. This feature of the Sohrab solver reduces the total running time of the FVM computation from the viewpoint of the programming of the code.

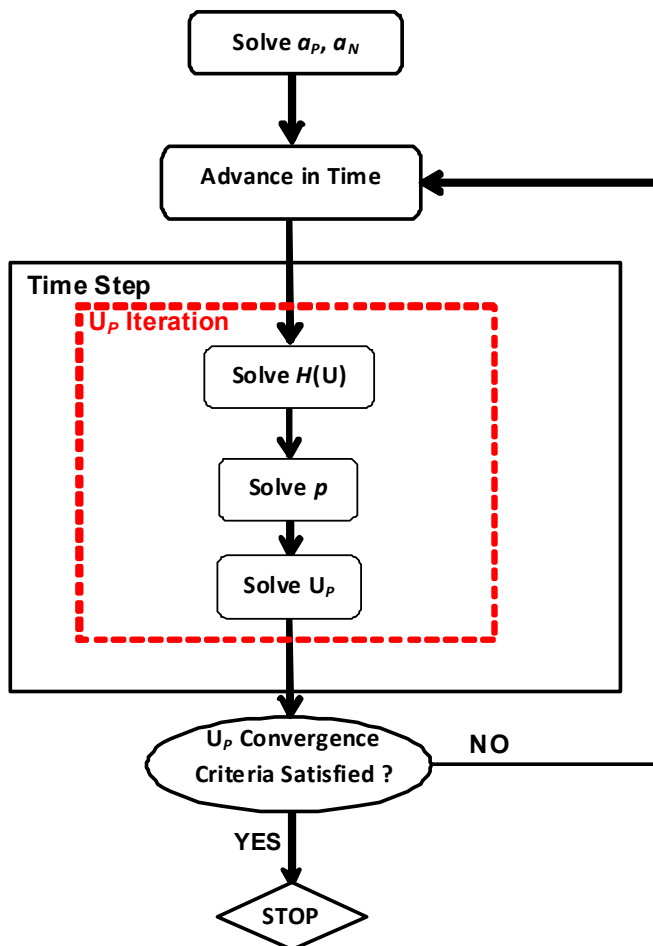


Figure 4. Flow chart of the calculation process of

The stability of a numerical solver is related to the Peclet number. It is defined as the ratio of the rate of advection to the rate of diffusion. For the Sohrab solver, the result is as follows:

$$Pe_{Sohrab} = \frac{\mathbf{w}}{\nu / \delta x} \quad (50)$$

where the convective velocity replaces the local velocity.

This result is different to the classical one of the Navier-Stokes solver, which can be expressed as:

$$Pe_{NS} = \frac{\mathbf{U}}{\nu / \delta x} \quad (51)$$

In order to preserve the stability of the FVM computation, the Peclet number is limited as:

$$Pe \leq 2 \quad (52)$$

Since  $\mathbf{w}$  is pre-constructed and kept as a constant during the FVM solving process, the Peclet number of the Sohrab solver will be more stable, while that of the Navier-Stokes will oscillate with  $\mathbf{U}$  oscillation because  $\mathbf{U}$  has to be updated in each time step. This comparison indicates that the Sohrab solver can reduce the numerical oscillation, and save the computational time further. In the following applications, this potential advantage will be proved by the numerical example.

#### 4.0 Application of the Sohrab solver: laminar boundary layer flow over a flat plate

In the sections before, the establishing process of the Sohrab solver has been discussed in detail. In this section, as the application of the Sohrab solver, an example of the laminar boundary layer flow over a flat plate will be computed. To give a validation to the code, the obtained results by the Sohrab solver will be examined by comparing them with the analytical solution of the modified equation of fluid motion, numerical solution obtained by the Navier-Stokes solver and the experimental results from literatures (Nikurades, 1942; Büttner and Czarske, 2005). These results comparisons would provide a valuable evaluation to the modified equation of fluid motion and the Sohrab solver.

#### 4.1 Analytical solution

For laminar flow over a flat plate, the analytical solution of the modified equation of fluid motion is available.



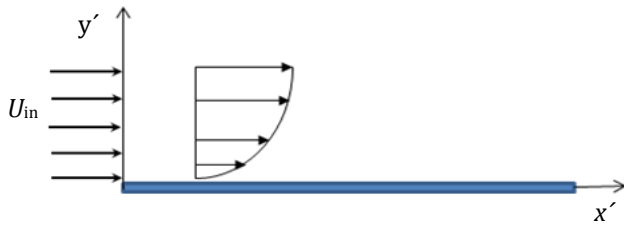


**Figure 5.** Laminar boundary layer flow over a flat

As discussed by Wan et al. (2009), the convective velocity for this flow model is uniform

$$\begin{aligned} w_x &= w_o \\ w_y &= 0 \end{aligned} \quad (53)$$

Then, define the dimensionless coordinates as

$$(x, y) = (x', y') / (v / w_o) \quad (54)$$

As an assumption for the analytical calculation, the boundary layer profile of this flow model can be simplified to a linear velocity profile (Inkman and Sohrab, 2008) as illustrated in Fig. 6. This approximation will be improved by the numerical iteration method later. On the basis of the assumption above, the convective velocity inside the laminar boundary layer, which is presented as an average velocity for the current flow model, can be simply defined as

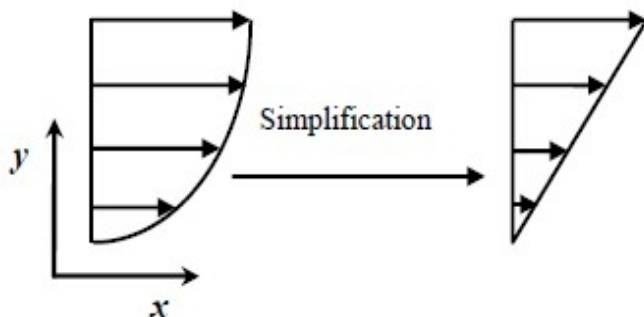


**Figure 6.** Laminar boundary layer simplification

Substituting Eq. (55) into the modified equation of fluid motion and making the usual boundary layer assumptions lead to the solution (Wan et al., 2009)

$$U / U_{in} = erf(\xi) \quad (55)$$

in terms of the similarity variable

$$\xi = \frac{y}{2\sqrt{2x}} \quad (56)$$

Hence the analytical solution of the modified equation of fluid motion for the velocity profile inside the laminar boundary layer can be expressed by an error function.

## 4.2 Numerical solution

As sketched in Fig. 7, a two-dimensional (2D) numerical computation model, including the entrance flow section and the flat plate, is built up for the laminar boundary layer flow test.

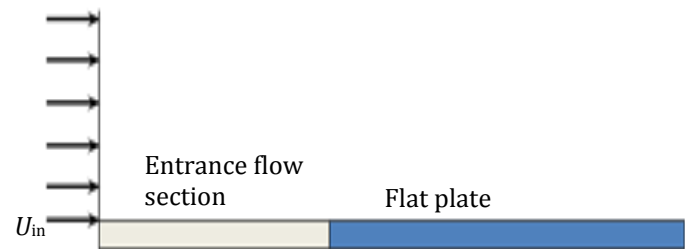


**Figure 7.** Numerical model of the laminar boundary layer flow over a flat plate

Corresponding to the numerical model in Fig. 7, the structured grids for the computational domain are shown in Fig. 8. After a grid-independent study is carried out, the grids number for the whole computational domain is about 5,000. In order to produce a smooth velocity profile inside the laminar boundary layer, a finely graded mesh is plotted next to the flat plate, followed by a more coarsely graded mesh above.

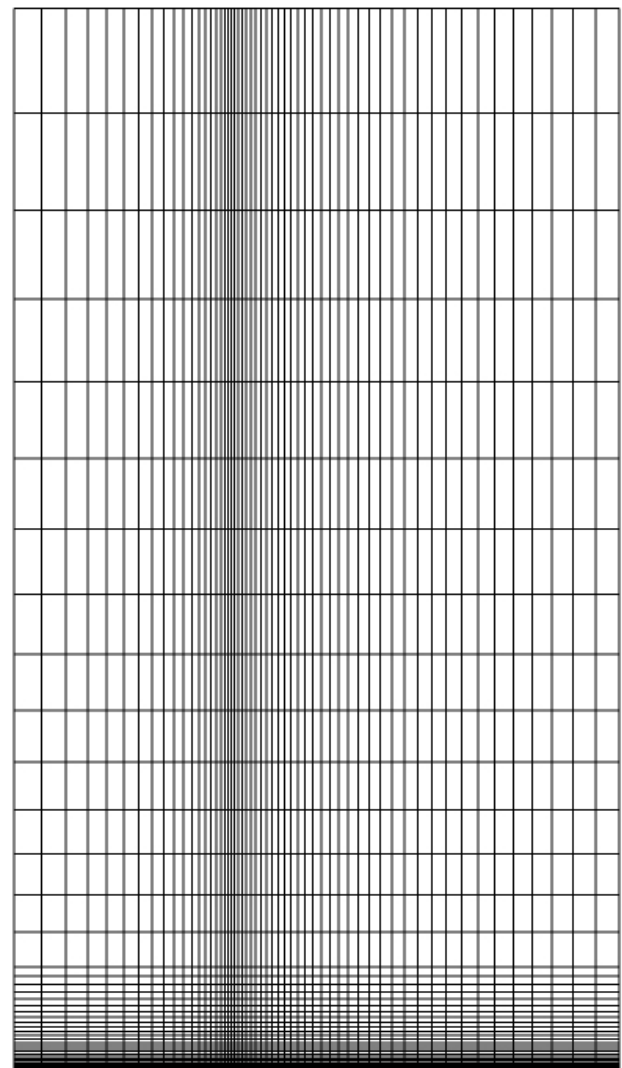


**Figure 8.** Grids of the laminar flow over a flat plate

Using the same convective velocity setup shown in Eq. (55), we obtain the numerical solution for the current flow model by the Sohrab solver. The resulted velocity profile is compared with the analytical solution. As shown in Fig. 9, the numerical result points follow the analytical solution exactly. This result demonstrates that the Sohrab solver developed in the current paper can precisely produce the numerical solution for the modified equation of fluid motion.

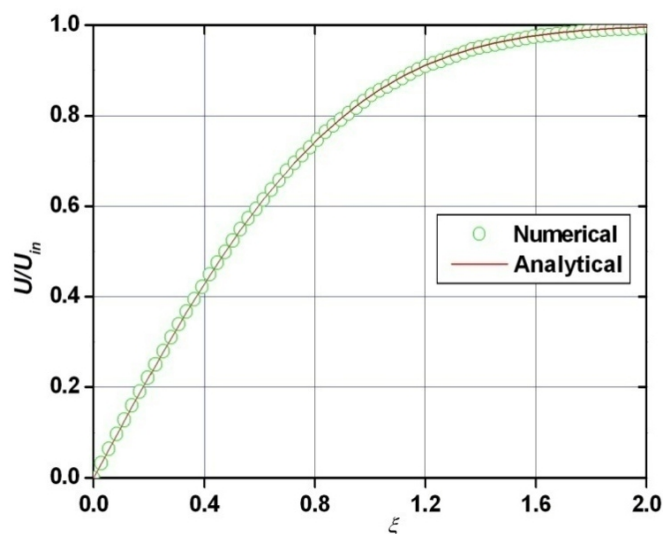


Figure 9. Comparison of the numerical and

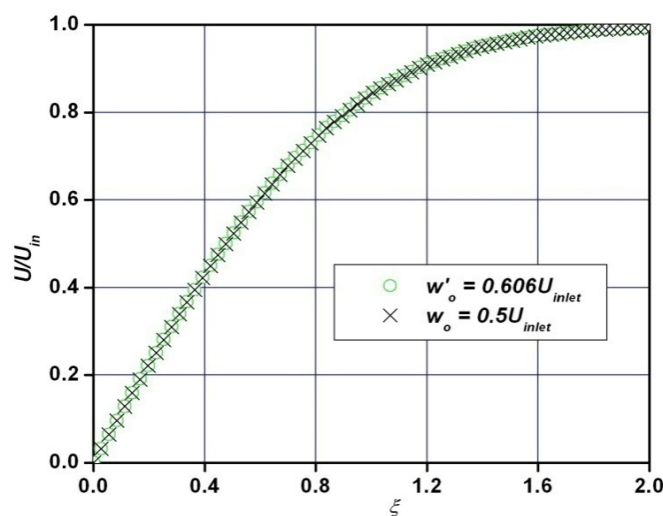


Figure 10. Comparison of the numerical solution

Noting the simplification in Fig. 6, we see that the solution for the convective velocity (Eq. (55)) may be slightly defective because of the linear assumption. As discussed by Inkman and Sohrab (2008), this assumption could be improved by averaging the resulted velocity profile in Fig. 9, making a new average convective velocity and solving the modified equation again for the velocity. This process can be iterated by using the developed numerical code. When the solution converges, the new result of the convective velocity is

$$w_o' = 0.606 U_{in} \quad (58)$$

Then the updated new velocity profile is compared with the old result which is under the assumption of Eq. (55). As presented in Fig. 10, after the convective velocity iteration is carried out, the updated velocity profile is almost identical to the old one. This comparison demonstrates that the convective velocity deviation influence is negligible for the modified equation of fluid motion and the assumption of Eq. (55) satisfies both the analytical and numerical solutions. Using the same boundary conditions and grids, we also applied the Navier-Stokes solver to resolve the current laminar flow model.

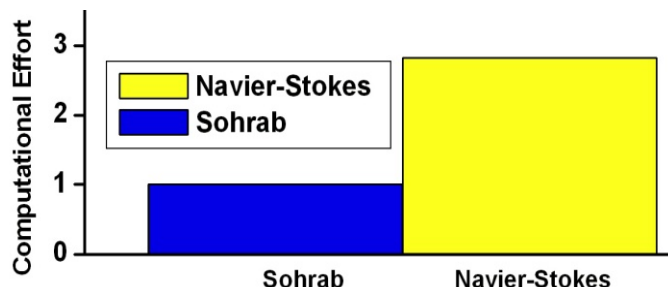


Figure 11. Comparison of the computational effort

The computational effort (or computational time) of the two solvers is compared in Fig. 11. Obviously, the Sohrab solver consumes much less time than the classical Navier-Stokes. This result offers the evidence in support of the analysis in section 3.2. The developed iteration technique in the Sohrab solver exerts the linear advantage of the modified equation of fluid motion to accelerate the numerical solution.

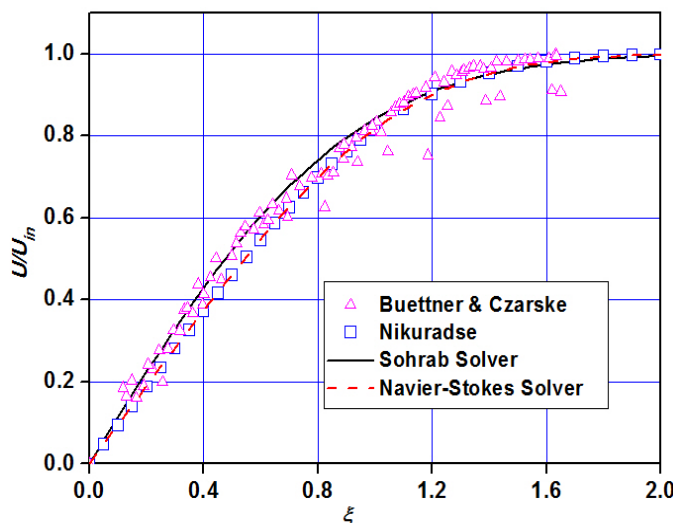


Figure 12. Comparison between the experimental data and numerical results

The resulted velocity profiles obtained by the both numerical solvers are compared with the experimental data including the well known results of Nikuradse (1942) and the recent laser Doppler interferometry measurement of Büttner and Czarske (2005). As shown in Fig. 12, the prediction of the Sohrab solver has a close agreement with the other three velocity profiles. In detail, the Sohrab solver result conforms more closely to the experimental data of Büttner and Czarske (2005), while the Navier-Stokes solver result exactly follows that of Nikuradse (1942). In the laser experimental results reported by Büttner and Czarske



(2005), deviation of the few velocity points from the other results can be found. As discussed by Büttner and Czarske (2005), this deviation is caused by an obstacle (a wire with 1 mm diameter) which was placed upstream on the glass plate and induced a turbulence. Therefore the Sohrab solver indeed provides a satisfied accuracy for the current laminar boundary layer flow problem, although it cannot replace the Navier-Stokes solve, the results of which matches measurement data perfectly. For this laminar boundary layer problem, more interesting comparisons between the modified equation results and the diverse measurement data can be found in Inkman and Sohrab (2008).

## 5.0 Conclusions

In the current paper, the derivation of the modified equation of fluid motion, which owns the linear properties, is discussed in detail. Based on this equation, a newly developed solver, termed the Sohrab solver, is introduced for CFD applications. The FVM discretisation process of the Sohrab solver is compared with that of the classical Navier-Stokes to highlight the linear advantage in theorem. Then, the Sohrab solver is applied to a basic laminar flow model to examine its accuracy and efficiency. The solution is validated by the analytical solution, experimental data (Nikuradse, 1942; Büttner and Czarske, 2005) and the numerical solution obtained by the classical Navier-Stokes solver. The interesting result indicates that both the Navier-Stokes solver and experiment support the Sohrab solver. The comparison also shows that the developed Sohrab solver is able to provide the exact solution for the modified equation of fluid motion. In terms of the conceptual linear advantages over the classical Navier-Stokes, the Sohrab solver requires less than half the computational time of the Navier-Stokes solver. All these comparisons demonstrate the scientific value of the Sohrab solver for the application of engineering flow problems. In addition, the turbulent flow problems have also be investigated by the Sohrab solver.

The associated results will be published in the following papers. Because of the encouraging results obtained for the fluid dynamic problem under current investigation, the described new numerical solver offers further evidence for the finite-volume method to solve the modified equation of fluid motion.

## Acknowledgment

The authors are very grateful to Prof. Siavash Sohrab, Northwestern University, IL for his support and contribution to this paper with helpful discussions.

## Nomenclature

|         |                       |
|---------|-----------------------|
| $A$     | Area                  |
| $a, a'$ | Velocity coefficient  |
| $D$     | Thermal viscosity     |
| $F$     | Force                 |
| $f$     | Distribution function |
| $k$     | Boltzmann constant    |
| $m$     | Mass                  |
| $n$     | Number                |
| $Pe$    | Peclet number         |
| $p$     | Pressure              |
| $p'$    | Kinematic pressure    |

|                    |                                      |
|--------------------|--------------------------------------|
| $r$                | Position                             |
| $t$                | Time                                 |
| $T$                | Temperature                          |
| $U$                | Element velocity, local velocity     |
| $u$                | Atom velocity                        |
| $v_{gh}, v_g, v_h$ | Diffusion velocity                   |
| $v'$               | Peculiar velocity                    |
| $w$                | System velocity, convective velocity |
| $x, y, z$          | Coordinates                          |
| $\delta$           | Distance                             |
| $\varepsilon$      | Potential energy                     |
| $\mu$              | Dynamic viscosity                    |
| $\nu$              | Kinematic viscosity                  |
| $\rho$             | Density                              |
| $\sigma$           | Stress tensor                        |
| $\psi$             | Invariant function of velocity       |

## Subscripts

|              |                  |
|--------------|------------------|
| $\beta$      | Scale of cluster |
| $E, N, P, W$ | Cell center      |
| $e, w$       | Node             |
| $In$         | Inlet            |
| $N-S$        | Navier-Stokes    |

## Abbreviations

|          |                                       |
|----------|---------------------------------------|
| 1D       | One-dimensional                       |
| 2D       | Two-dimensional                       |
| CFD      | Computational fluid dynamics          |
| FVM      | Finite volume method                  |
| LHS      | Left hand side                        |
| OpenFOAM | Open field operation and manipulation |
| RHS      | Right hand side                       |

## References

1. Benra FK and Sohrab SH (2006). Modified theories of laminar flow around a rigid cylinder and flow outside and inside a liquid cylinder in uniform and counterflow gaseous jets. WSEAS Trans. Fluid Mech. 1: 533-542.
2. Büttner L and Czarske J (2005). Investigation of the influence of spatial coherence of a broad-area laser Diode on the interference fringe system of a Mach-Zehnder interferometer for highly spatially resolved velocity measurement. Applied Optics. 44: 1582-1590.
3. Golse F (2011). From the kinetic theory of gases to continuum mechanics. AIP Conf. Proc. American Institute of Physics. 1333, pp. 15-27.
4. Inkman MJ and Sohrab SH (2008). Comparisons between velocity profiles according to the modified and the Navier-Stokes equations of motion and the experimental measurements for laminar boundary layer over a flat plate. Proc. 12th WSEAS Int. Conf. on Computing and Computational Techniques in Sciences, Maza et al., eds., WSEAS Press, Athens, pp. 116-124.
5. Jasak H (1996). Error analysis and estimation for the finite volume method with application to fluid flows. Ph. D. Thesis, Imperial College, London
6. Nikurades J (1942). Laminare Reibungsschichten an der längsangetrönten Platte. Monograph, Zentrale f. Wiss. Berichtswesen, Berlin.
7. Patankar SV (1980). Numerical Heat Transfer and Fluid Flow. Hemisphere, Washington, DC.

8. Sohrab SH (1999a). A scale-invariant model of statistical mechanics and modified forms of the first and the second laws of thermodynamics. *Int. J. Therm. Sci.* 38: 845-853.
9. Sohrab SH (1999b). Modified form of the equation of motion and its solution for laminar flow over a flat plate and through circular pipes and modified Helmholtz vorticity equation. *Chemical and Physical Processes in Combustion, Fall Technical Meeting, The Eastern States Section*, pp. 375-378.
10. Sohrab SH (2005). A modified theory of laminar flow near a rotating disk. *IASME Transactions.* 2: 152-160.
11. Sohrab SH (2008a). A modified scale invariant statistical theory of turbulence. *Proc. 6th IASME/WSEAS Int. Conf. On Fluid Mechanics (FMA'08)*, Rhodes, Greece.